Block interleaver dimensioning and real-time demonstration for ground-to-satellite optical communications

Daniel Romero Arrieta, Almonacil Sylvain, Jean-Marc Conan, Laurie Paillier, Vincent Michau, Eric Dutisseuil, Sébastien Bigo, Jérémie Renaudier, Rajiv Boddeda

Block Interleaver Dimensioning and Real-Time Demonstration for Ground-to-Satellite Optical Communications

Daniel Romero Arrieta[1,2], Sylvain Almonacil[1], Jean-Marc Conan[2], Laurie Paillier[2], Vincent Michau[2], Eric Dutisseuil [1], Sébastien Bigo[1], Jérémie Renaudier[1], Rajiv Boddeda[1]

[1] Nokia Bell Labs, Route de Villejust, 91620 Nozay, France, daniel.romero_arrieta@nokia.com
[2] ONERA, DOTA, Paris Saclay University, F-92322 Châtillon

Abstract *We provide a methodology to dimension the interleaver duration for free-space optical links. We validate it on an FPGA transceiver by emulating ground-geostationary strong turbulence conditions. 150ms interleaver reduces launch power by two orders of magnitude, making it compliant with commercially-available amplifiers to transmit 10Gbit/s.*

Introduction

The continuous increase in the demand for data transmission has pushed the state-of-the-art radio frequency satellite links to their theoretical ceiling. Optical ground-satellite links can bring a large capacity leap but suffer from channel specific impairments, such as frequency selective molecular absorption [1,2], cloud attenuation and atmospheric turbulence induced power variations. The refractive index variations due to turbulence create time-distributed attenuation peaks of received optical power (ROP). Due to the finite receiver sensitivity and the optical amplifier output power limitations (few tens of watts [3]), the attenuation peaks create error bursts. These bursts can be partially mitigated by time diversity techniques [4] but at the expense of duplicating the communication hardware. A more promising approach is to use Adaptive Optics (AO) [5], complemented with channel encoding and a data interleaver [6,7].

In this article, we propose a methodology for dimensioning a block interleaver for that purpose. As a case study, we consider a ground to geostationary (GEO) satellite uplink while accounting for point-ahead anisoplanatism [5] in strong turbulence. We use a numerical tool to generate time series of the received optical power after adaptive optics pre-compensation and ground-satellite propagation. We then apply the proposed methodology to assess the required interleaver duration to ensure that the errors after the deinterleaver are adequately distributed. Finally, we validate the technique experimentally by emulating a 10 Gbit/s free space optical chain incorporating a real-time interleaving system on FPGAs.

Dimensioning Block Interleavers

In Fig.1a, we depict an uplink communication system through the atmosphere along with data encoding and decoding blocks. The blocks in solid line are implemented experimentally except for the FEC coding and codeword interleaving (π) to correct residual bursts (~100s bits).

As the Forward Error Correction (FEC) blocks cannot correct burst errors of ~ms, interleaving is used to distribute the errors over a long duration, called the interleaver time. Here we use a block interleaver with M rows and N columns [8]. As it is impractical to implement bit per bit interleavers at high data rates, we consider an interleaver which interleaves blocks of bits. We denote I_{res} the number of bits per block, as shown in Fig. 1b. The input/output blocks are written/read in/from the columns/rows of the matrix, respectively. At the reception, the received bits are deinterleaved and forwarded to the error correction stage.

Without loss of generality, we assume that any interleaver matrix contains e_b burst errors while the other bits have a mean bit error rate (BER) of $\overline{BER}$. To distribute the errors uniformly over all the FEC codewords in the interleaver matrix, we set the value of M as follows

$$\mathrm{M} = \left\lceil \frac{FEC_N}{I_{res}} \right\rceil \qquad (1)$$

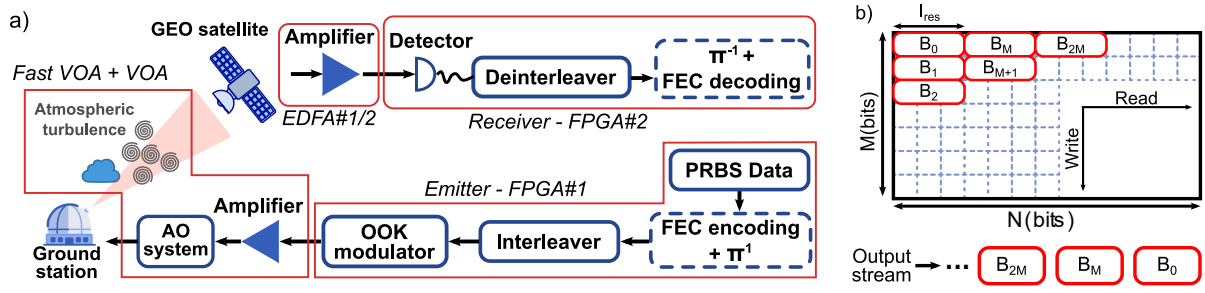

Fig. 1: (a) The optical communication chain for ground-satellite communication, solid line blocks were experimentally emulated. (b) MxN block interleaver with blocks of size I_{res} at the transmitter.

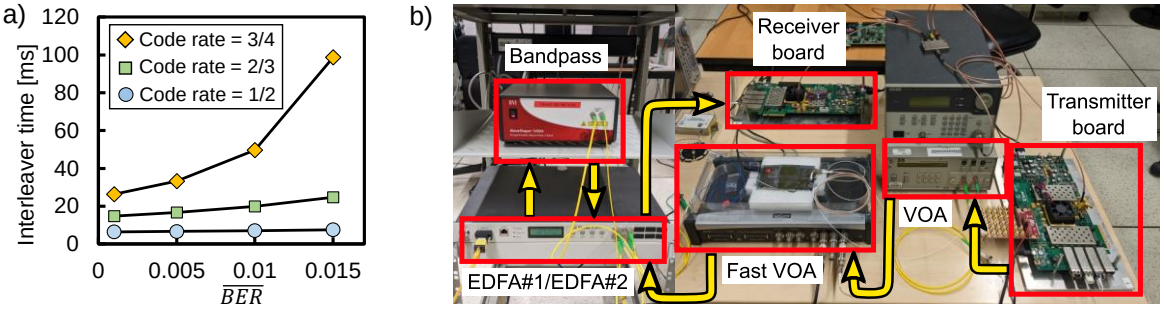

Fig. 2: (a) Interleaver time as a function of $\overline{BER}$ for different FEC code rates for a fading time of 1 ms. (b) The experimental apparatus emulating a free space optical link communication system.

Where FEC_N is the size of the FEC codeword and $\lceil . \rceil$ denotes the ceiling function. Assuming a continuous e_b, the maximum number of burst errors per FEC codeword is given by

$$e_{FEC_b} = I_{res} \times \left\lceil \frac{e_b}{N} \right\rceil \quad (2)$$

Assuming a constant $\overline{BER}$ for the remaining bits, the total number of errors per FEC codeword can be estimated using

$$e_{FEC} = e_{FEC_b} + \overline{BER}(FEC_N - e_{FEC_b}) \quad (3)$$

Thus, for a given FEC, with pre-FEC BER threshold of BER_{FEC}, N must satisfy the following condition

$$\text{N} \geq \left\lceil \frac{I_{res} \times e_b(1-\overline{BER})}{2FEC_N(\text{BER}_{FEC} - \overline{BER})} \right\rceil \quad (4)$$

Which is valid when $\overline{BER}$ is lower than BER_{FEC} threshold. For a bit rate of R_b, the interleaver time is given by $(M \times N)/R_b$. The ratio between the interleaver time and the fading time (eb/Rb) depends only on the FEC limit and the $\overline{BER}$. We consider the DVB-S2 standard's FEC as reference [9] ($FEC_N = 64800$) with hard decision decoding yielding pre-FEC BER limits of 0.08, 0.035, 0.02 for code rates 1/2, 2/3 and 3/4 at a post-FEC BER of 10^{-9}. In Fig. 2a, we present the interleaver time as a function of the $\overline{BER}$ for various code rates using a 1 ms fading time. As expected, higher code rates require longer interleaver times and we use a code rate of 1/2 as a baseline to minimize the interleaver length.

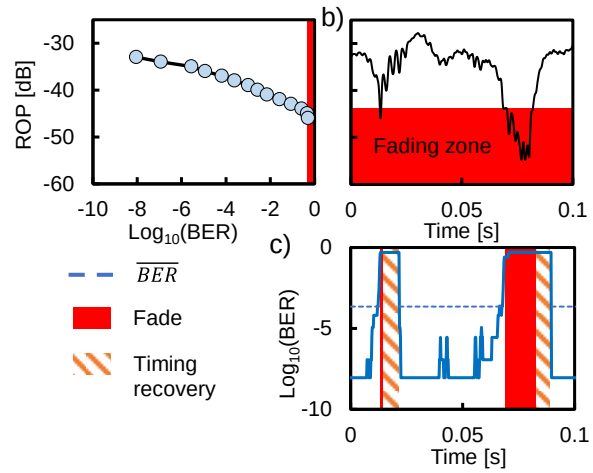

Fig.3: (a) The dependence of the measured BER with ROP. BER reaches 0.5 for ROP <-45 dBm (b) A snippet of a time series of 100 ms with the fading zone in red. (c) BER of the time series.

Channel modelling

In this section, we describe how we generate a representative set of timeseries expected in ground to geostationary satellite links to illustrate our methodology. In optical atmospheric propagation, the spatial strength of the atmospheric turbulence is characterized by two parameters: the coherence length (r_0 also called Fried parameter) and the anisoplanatic angle (θ_0). The smaller these values, the more severe the turbulence. We use the measurements presented in [10, 11] to generate turbulence profiles as show in [5]. Assuming r_0 and θ_0 as independent stochastic variables, we selected a turbulence profile which comprises 99.9% of the measured cases. We obtained a r_0 of 4 cm and a θ_0 of $4.8\ \mu rad$, along the line of sight at 1550 nm.

The temporal behaviour of the turbulence can be modelled by the vertical windspeed profile. Here as a challenging scenario, we selected a large windspeed at ground level ($10\ m/s$) which requires rapid adaptive optics response (4.7 kHz, ~0.5 ms delay correcting up to 90 Zernike radial modes in our simulations), while keeping low tropospheric windspeed ($15\ m/s$.) which creates long coherence times and large error bursts.

To obtain the received optical power time series we use an experimentally validated simulation tool [12], fed with the obtained wind and turbulence profiles. We generated multiple time series of 1 second duration for a ground to geostationary satellite link with a 40 and 25 cm emission and reception pupil, respectively, with the link budget model presented in [5].

Experimental measurements

We use an NRZ-OOK based transceiver for the optical modulation of the data at 10 Gbps. The experimental setup is shown in Fig. 2b. We implemented a real-time block interleaver and deinterleaver on two VC709 FPGA boards each

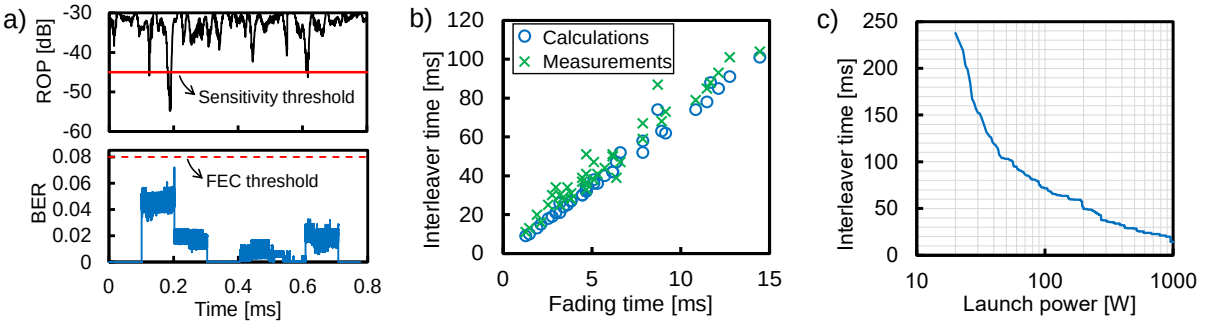

Fig.4: (a) The measured BER after the deinterleaver with all the received blocks below the FEC threshold (0.08). (b) The measured and calculated interleaver time for different fading times from the time series. (c) The minimum simulated interleaver time as a function of the launch power.

equipped with 1 DDR3 SDRAM memory [13] with a capacity of 32 Gbits and a data transfer rate of ~100 Gbps. At the transmitter, a pseudorandom binary sequence (PRBS) bit stream is generated and interleaved before modulation. We use $I_{res} = 512$ bits which is sufficiently small (< 1% of the FEC codeword) while allowing us to sufficiently expedite the memory write/read times. As the deinterleaver at the receiver needs to recover the exact position of the incoming data in the interleaving matrix, a frame with headers containing the block order information is created at the transmission. An additional 1% overhead is used for this synchronization.

The modulated signal is then sent to a variable optical attenuator (VOA) which emulates the static channel losses. Then, a fast VOA with a bandwidth (5 MHz) higher than the power variations (<1 kHz) is used to emulate the simulated timeseries. At the reception, the signal is pre-amplified using Erbium Doped Fiber Amplifier (EDFA) #1, filtered (50 GHz) to perform amplifier noise rejection and amplified by EDFA#2 to reach the power level required by the receiver photodiode. At its output, the bit stream is aligned, deinterleaved and uncoded BER is measured for each FEC codeword length.

In the static regime, the BER of the received data was measured as a function of ROP (Fig. 3a). We found that when the ROP falls below a threshold of -45 dBm the receiver loses the clock reference and typically recovers around ~0.7 ms after it rises above this threshold.

To calculate the interleaver time, we first estimate the fading time and the $\overline{BER}$ from the generated time series. To do this, we look for fadings in a 100 ms window as shown in Fig. 3b. Then, using the measured ROP to BER curve, we calculate the BER in the window and add the timing recovery as shown in Fig. 3c. The fading time corresponds to the segments which are shown in red (solid and line pattern) and the $\overline{BER}$ (dashed line) was calculated in the segments with BER less than 0.5. We found that $\overline{BER}$ typically lies within 0.001 and 0.01. By increasing the launch power at the transmitter and consequently the received power, the fading times decrease. Even for a launch power of 60 W, we observed that fading times vary between 1 and 15 ms.

We now measure experimentally the required interleaver time by varying the interleaver time until all the codewords after the interleaver have a BER lower than pre-FEC limit. In Fig. 4a, we show a snippet of the ROP series along with the measured BER in time after the de-interleaver. We observe that for the chosen interleaver time (100 ms) all the codewords satisfy the FEC condition. This whole process is repeated for each fading event and varying its position in the interleaver window. In Fig. 4b, we show the measured required interleaver times (crosses) for various fading times along with the calculated ones (blue circles). The measurements fall within +/-10% of the calculations in up to 95% cases. The residual error could be attributed to the presence of multiple fadings or fading position in the interleaver window for the measurements whereas the simulations were done by assuming the fading event in the middle of the window.

For various launch powers, we calculate the minimum interleaver time for the worst fading event over all the time series, and the results are shown in Fig. 4c. We can see that even for large launch powers an interleaver is necessary for error-free transmissions under strong turbulence. We observe that an interleaver of 150 ms can bring a reduction of two orders of magnitude, making it feasible to use a commercially available amplifier of 30 W [14] to establish 10 Gbps links.

Conclusion

In this article, we proposed a methodology for dimensioning the block interleaver size for optical satellite links. We developed a real-time FPGA interleaver and validated our methodology under strong turbulence conditions. The predictions agree within +/- 10% with the measurements. With commercial amplifiers, we showed that an interleaver of 150 ms is sufficient to transmit 10 Gbps ground-geostationary satellite links.

References

[1] D. R. Arrieta, R. Boddeda, S. Almonacil, T. Allain, and S. Bigo, “Capacity Limits of Optical Satellite Communications,” *European Conference on Optical Communication (ECOC)*, Dec. 2020, doi: 10.1109/ECOC48923.2020.9333284.

[2] S. Almonacil, R. Boddeda, and S. Bigo (2021). “Experimental Study of the Impact of Molecular Absorption on Coherent Free Space Optical Links”, *European Conference on Optical Communication (ECOC) 2021*, doi:10.1109/ECOC52684.2021.9606172

[3] O. Varona, M. Steinke, J. Neumann, D. Kracht, “All-fiber, single-frequency, and single-mode Er^{3+}:Yb^{3+} fiber amplifier at 1556 nm core-pumped at 1018 nm”, *Opt Lett.* 2018 Jun 1;43(11):2632-2635. doi:10.1364/OL.43.002632.

[4] S. Trisno, I. I. Smolyaninov, S. D. Milner, and C. C. Davis, “Characterization of time delayed diversity to mitigate fading in atmospheric turbulence channels”, 2005 doi:10.1117/12.617645

[5] N. Vedrenne, C. Petit, A. Montmerle-Bonnefois, C. B. Lim, J.-M. Conan, L. Paillier, M.-T. Velluet, K. Caillault, F. Gustave, A. Durecu, V. Michau, F. Cassaing, S. Meimon, J. Montri, "Performance analysis of an adaptive optics based optical feeder link ground station," *Proc. SPIE 11852, International Conference on Space Optics* (ICSO), 1185219, 2020.

[6] Y. Q. Shi, Xi Min Zhang, Zhi-Cheng Ni and N. Ansari, "Interleaving for combating bursts of errors," in *IEEE Circuits and Systems Magazine*, vol. 4, no. 1, pp. 29-42, 2004, doi:10.1109/MCAS.2004.1286985.

[7] J. A. Greco, "Design of the high-speed framing, FEC, and interleaving hardware used in a 5.4km free-space optical communication experiment," *Proc. SPIE 7464, Free-Space Laser Communications IX*, 746409, 2009.

[8] A. Kenneth, C. Heegard, and D. Kozen. “A Theory of Interleavers”, *Technical Report.* Cornell University, USA, 1997.

[9] JTC, “EN 302 307-1 - V1.4.1 - Digital Video Broadcasting (DVB); Second generation framing structure, channel coding and modulation systems for Broadcasting, Interactive Services, News Gathering and other broadband satellite applications; Part 1: DVB-S2,” France, 2014.

[10] D. Sprung, and E. Sucher, “Characterization of optical turbulence at the solar observatory at the Mount Teide”, Tenerife. *Proc. SPIE 8890, Remote Sensing of Clouds and the Atmosphere XVIII; and Optics in Atmospheric Propagation and Adaptive Systems XVI, 889015,* 2013, doi:10.1117/12.2032744

[11] J. Osborn, R. W. Wilson, M. Sarazin, T. Butterley, A. Chacón, F. Derie, O. J. D. Farley, X Haubois, D. Laidlaw, M. LeLouarn, E. Masciadri, J. Milli, J. Navarrete, M. J. Townson, “Optical turbulence profiling with Stereo-SCIDAR for VLT and ELT” *Monthly Notices of the Royal Astronomical Society*, *478*(1), 825–834, 2018, doi:10.1093/MNRAS/STY1070

[12] N. Védrenne, M. T. Velluet, M. Séchaud, J. Conan, and M. Toyoshima, “Turbulence effects on bi-directional ground-to-satellite laser communication systems,” in *International Conference on Space Optical Systems and Applications (ICSOS)*, 2012.

[13] *DDR3 SDRAM STANDARD | JEDEC*. (n.d.). Retrieved May 9, 2022, from https://www.jedec.org/standards-documents/docs/jesd-79-3d

[14] ELR-SF Erbium Single-frequency CW Lasers. (n.d.). Retrieved May 10, 2022, from https://www.ipgphotonics.com/en/products/lasers/low-power-cw-fiber-lasers/1-53-1-65-micron/elr-sf-1-30-w